**FACTA UNIVERSITATIS**
Series: **Electronics and Energetics** Vol. 27, N$^{o}$ 2, June 2014, pp. 205 - 219
DOI: 10.2298/FUEE1402205H

# DEMONSTRATION OF PROTEIN HYDROGEN BONDING NETWORK APPLICATION TO MICROELECTRONICS

**Marin H. Hristov[1], Rostislav P. Rusev[2], George V. Angelov[1], Elitsa E. Gieva[1]**

[1]Technical University of Sofia/Department of Microelectronics, Sofia, Bulgaria
[2]Technical University of Sofia/Department of Technology and Management of Communication Systems, Sofia, Bulgaria

**Abstract**. *Model of hydrogen bonding networks in active site of β-lactamase during the last intermediate EY of acylenzyme reaction semicycle is presented. The I-V characteristics of each hydrogen bond are calculated following Marcus theory and theory of protein electrostatics. Simulations showed that HBN characteristics are similar to the characteristics of microelectronic devices such as amplifier, signal modulator, triangular pulse source. The results demonstrated the analogy of HBNs in the active site of β-lactamase protein to microelectronic integrated circuit with multiple outputs each with different characteristics*.

**Key words**: *bioelectronics, microelectronics, proteins, hydrogen bonding networks, β-lactamse, acylenzyme reaction, proton transfer*.

## 1. INTRODUCTION

Bioelectronics is a relatively new field associated with the integration of biomolecules with electronic elements to yield functional devices. The first molecular materials used in electronics originate from material science and are related to the development of electronic and optoelectronic devices that utilize the macroscopic features of organic compounds. The remarkable biochemical and biotechnological progress in tailoring new biomaterials by genetic engineering or bioengineering provides unique and novel means to synthesize new enzymes and protein receptors, and to engineer monoclonal antibodies for nonbiological substrates (such as explosives or pesticides) and DNA-based enzymes. All these materials provide a broad platform of functional units for their integration with electronic elements. After many years of research, the organic light-emitting devices, synthetic electronic circuits, chemical and biochemical sensors have drawn attention.

Molecular scale devices attract substantial research efforts because of the basic fundamental scientific questions and the potential practical applications of the systems. In

Received January 20, 2014
**Corresponding author:** George V. Angelov
Technical University of Sofia/Department of Microelectronics, Sofia, Bulgaria
(e-mail: angelov@ecad.tu-sofia.bg)

particular, efforts are focused on single molecule behavior or behavior of group of molecules and precise 3D position control over single atoms and molecules. The major activities in the field of bioelectronics relate to the development of biosensors that transduce biorecognition or biocatalytic processes in the form of electronic signals [1], [2], [3]. There are certain applications of bioelectronics molecular structures in switches, DNA and other molecular devices that could be implemented in standard solid-state silicon electronics [4]; such molecule structures that could become real competitor to state-of-the-art silicon microelectronic devices. Other research efforts are directed at utilizing the biocatalytic electron transfer functions of enzymes to assemble biofuel cells that convert organic fuel substrates into electrical energy [5], [6]. Exciting opportunities exist in the electrical interfacing of neuronal networks with semiconductor microstructures. The excitation of ion conductance in neuronsmay be followed by electron conductance of semiconductor devices, thus opening the way to generating future neuron-semiconductor hybrid systems for dynamic memory and active learning [7].

One goal of molecular electronics is to imitate complex process behavior of solid-state circuits in molecular structures that would allow for creation of bioelectronics devices. Biological molecules – namely enzymes, proteins, and DNA – are unique, in that they have benefited from natural selection and evolution, which has resulted in highly optimized properties custom-tailored for specific biological functions. These molecules have evolved to function in a wide range of environmental conditions, often with efficiencies unmatched by nonbiological or synthetic methods. Rational selection by the researcher can bring their novel functionalities to device applications.

From the standpoint to application of bioobjects to devices that are similar to conventional microelectronics devices proteins are widely sensitive to the presence of many types of molecules, through both specific and nonspecific binding. This is especially true for enzymes, which participate in a large variety of specific interactions with small molecules. The primary result is conformational modification of the protein, resulting in a change of activity. Molecules that interact with proteins through nonspecific or indirect interactions typically disrupt noncovalent bonds which in turn alter structure. The challenge here is to detect these changes and transform them into signals that can be processed analogous to solid-state microelectronic devices.

For certain classes of proteins, e.g. photoactive yellow protein (PYP) [8], green fluorescence protein [9], bacteriorhodopsin [10], the problem with signal formation and processing is simpler because these proteins can produce (or at least can be made to produce) a measurable response that can be sensed into the form of a signal.

The understanding of charge transport phenomena through biological structures is essential for the problem of signal formation. It is constantly evolving due to the intensive theoretical and experimental work. The contributions of the Marcus theory [11], the super exchange charge transfer theory [12], and the definition of superior tunneling paths in proteins [13] had an enormous impact on the understanding of biological processes in numerous electrochemical and photoelectrochemical biosensing systems.

Bacteriorhodopsin (bR) has drawn a large amount of attention from the perspective of both the basic and applied sciences. It is a unique protein because it acts as a light-driven engine that converts light into chemical energy in an efficient manner. Bacteriorhodopsin possesses hydrogen bonding networks that executes **proton transport**. This implies that

proteins with its hydrogen bonding networks (HBN) can process information. Such protein with hydrogen bonding networks is $\beta$-lactamase [14].

In this paper, we demonstrate the application of HBNs in the active site of $\beta$-lactamase protein as analog to microelectronic integrated circuit with multiple outputs each with different characteristics.

## 2. HBN MODELING APPROACH

Signal transfer in hydrogen bonding networks (HBNs) is carried out by protons. The model of proton transfer in hydrogen bonds is based on Marcus theory and the protein electrostatic theory [15]. Proton current in the hydrogen bonds depends on the value of pH. Changing the pH causes polarization and ionization of the protein groups. In result, the charges in protein-water system are redistributed and the donor/acceptor electrostatic potentials change. The proton transfer parameter (respectively proton current) between changes as well.

In analogy to traditional microelectronic four-terminal elements, where the input circuit correlates to the output circuit and the electrical current itself is formed by electrons, some protein hydrogen bonds that are connected in a HB network could be modeled as four terminal block-elements; the current in each block-element is formed by a transfer of protons between donor and acceptor parts of the heavy atoms in the network [16]. This analogy allows us to model HBNs with four terminal circuit block-elements. The *I-V* characteristics of each block-element are proportional to the *K-V* characteristics of the respective hydrogen bonds. The current (*I*) of each block-element represents the proton transfer parameter (*K*) of each hydrogen bond and the voltage (*V*) of each block-element represents the electrostatic potential (El. pot.) [16].

### 2.1. Types of HBNs studied

In our earlier research in the field of bioelectronics so far [17]-[21], we have investigated $\beta$-lactamase protein and in particular, its hydrogen bonding networks (HBNs). We have examined different types of HBNs including branching HBNs, linear HBN with protein residues and water molecules, HBN from protein main chain, and HBN in active site of protein. We have compared hydrogen bonds characteristics to the characteristics of various well-known electronic elements such as transistors, amplifiers, filters, currents sources, decoders, etc.

Branching network is depicted in Fig. 1. Linear networks with and without water molecule are given in Fig. 2.

These hydrogen bonding networks (HBN) extracted from $\beta$-lactamase, consist of residues in the periphery of the protein and water molecules. B. Atanasov et. al [22] assume that proton transfer in the active site HBNs of the $\beta$-lactamase is performed during the interaction of the protein with the *ligand* (acylenzyme reaction).

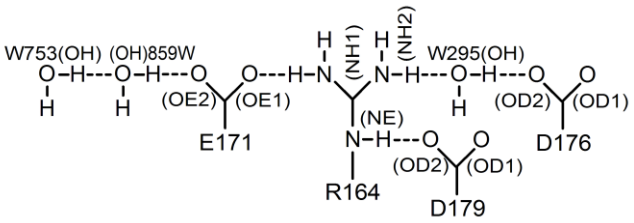


**Fig. 1** Hydrogen Bonding Network. NH1, NH2, and NE — nitrogen atoms of arginine residue R164, OE1 and OE2 — carboxyl oxygen atoms of glutamic acid residue E171, OD1 and OD2 - carboxyl oxygen atoms of Aspartic acid residues, OH — are oxygen atoms of water molecules (W295, W753 and 859W)

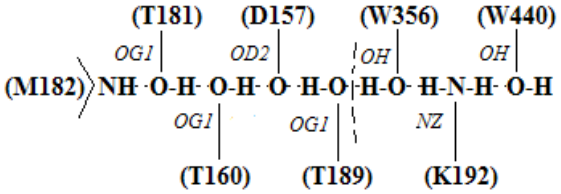


**Fig. 2** Hydrogen bonding network is virtually separated into two parts (with dashed line). (M182) is methionine residue, OG1 is hydroxyl oxygen of threonine residues (T160, 181, 189), OD2 is carboxyl oxygen of aspartic acid residue (D157), NZ is nitrogen atom of lysine residue (K192), OH is oxygen atom of water molecules (W356, 440)

### 2.2. Acylenzyme reaction

The HBNs in the active site of $\beta$-lactamase protein during acyl enzyme reaction is given in Fig. 3. There are two HBNs participating in the acylenzyme reaction. The first HBN, referred to as **nucleophilic**, consists of residues S70, w297, N170, E166, K173, N132. The second HBN, referred to as **electrophilic**, consists of S130, K234, w309, D214, S235. It should be noted that there is proton transfer in parallel in both the two HBNs during the different intermediates of the reaction.

Acyl enzyme reaction cycle has the following intermediates: (E) the networks in the active site of the free enzyme, (ES) the formation of Michaelis complex, (T1) the transient state of reaction where the networks change due to the nucleophilic attack by S70, (EY) the end of the reaction when the acylenzyme is formed up and the networks of hydrogen bonds have changed due to the opening of the ligand ring and the combination of the ligand with S70.

The catalyzed $\beta$-lactam nitrogen protonation is supposed to be energetically favored at the initiating event, followed by nucleophilic attack on the carbonyl carbon of the $\beta$-lactam group. Nitrogen protonation is catalyzed through a hydrogen bonding network involving the 2-carboxylate group of the substrate, S130 and K234 residues, and a water molecule. The nucleophilic attack on the carbonyl carbon is carried out by the S70 with de- protonation abstraction catalyzed by a water molecule hydrogen-bonded to the side chain of E166.

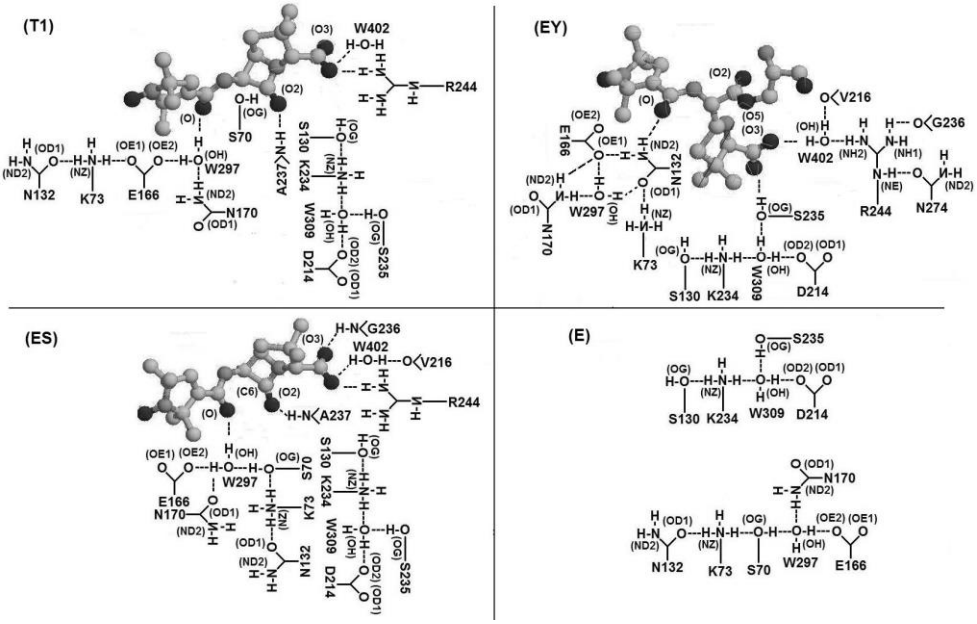


**Fig. 3** Acylenzyme reaction intermediates – HBNs in the active site of: (E) free enzyme, (ES) Michaelis complex, (T1) transient state, (EY) acyl enzyme. The first HBN is referred to as "nucleophilic" consists of residue S70, water molecule w297, and residues N170, E166, K173, N132 and ligand. The second referred to as "electrophilic" consists of consists of residues S130, K234, water molecule w309, and residues D214, S235

Proton transfer between donor and acceptor of each hydrogen bond in protein is studied following Marcus theory. Proton transfer parameter $K$ is calculated by

$$K = \frac{k_B T}{2\pi} \exp\left( -\frac{Eb - h\omega/2}{k_B T} \right) \tag{1}$$

where $k_B$ – Boltzmann constant, $Eb$ – barrier energy, $h$ – Plank constant, $\omega$ – frequency, $T$ – temperature in Kelvins.

The energy barrier is calculated by:

$$\begin{aligned} Eb &= (s_A(R(DA) - t_A)^2 + v_A) + s_B E_{12} \\ &+ (s_C \exp(-t_C(R(DA) - 2)) + v_C)(E_{12})^2 \end{aligned} \tag{2}$$

where $R(DA)$ – distance between donor and acceptor, $E_{12}$ – the difference between the energies of donor and acceptor (cf. two-well potential).

$K$ has dimension of free energy and from the calculations, it can be interpreted as follows: the greater parameter $K$ – so much readily accomplished proton transfer between donor and acceptor from HBNs, i.e. the proton current will be greater. On the other hand, the parameter of

proton transfer depends on the donor/acceptor potentials similarly to the potentials supplying the microelectronic components. Therefore we can construct three and four-terminal electronic block-elements analogous to the hydrogen bonds in the following way.

The electrostatic potential of each protein atom is calculated by protein electrostatic theory. Both *K* parameter and electrostatic parameter depend on pH of the environment.

It is observed that the electrostatic potential of donor/acceptor of each hydrogen bond could be compared to the voltage of a conventional microelectronic circuit device. Proton transfer parameter *K* could be compared to the circuits' device current.

This lets us introduce the analogy between hydrogen bonds and standard microelectronic devices, respectively HBNs and microelectronic circuits. In particular, we will study the behavior of block-elements circuits, modeled with polynomials, in Matlab [23]. Afterwards, the Matlab simulations with polynomials are compared to the results of simulations obtained using Marcus theory in [24].

## 3. CIRCUIT MODEL

### 3.1. Circuit formulation

We create circuit *block-elements* corresponding to each HBN in order to emulate the operation of HBNs. HBN is divided in heavy atoms that form the hydrogen bonds (Fig. 4).

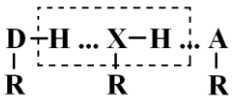


**Fig. 4** Sample HBN with its heavy atoms X, D, and A

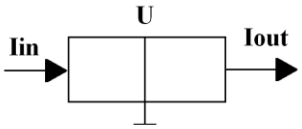


**Fig. 5** Block-element that is analogous to heavy atom from the hydrogen bonding network

In the analogous circuit each heavy atom (which is both donor and acceptor, designated with 'X') is represented as a separate block-element (Fig. 5).

In Fig. 5 the acceptor part of the heavy atom 'X' is assigned as the input of the respective block-element where the input current $I_{in}$ flows in; the donor part of the heavy atom 'X' is assigned as the output of the respective block-element, where the output current $I_{out}$ flows out. The potentials at the input and the output of the block-element are equal to the potential *U* of the heavy atom. The magnitude of the input and output currents are proportional to the proton transfer parameter of the hydrogen bonding network where the heavy atom is present.

In each protein HBN we can find strong proton donor, strong proton acceptor, and atoms exhibiting both donor and acceptor properties. Strong proton donor of each HBN always behaves as circuit input and strong acceptor of each HBN always behaves as circuit output.

We consider the application of the HBN properties on the example of hydrogen bonding network in active site during the intermediate of acyl enzyme reaction (case EY

of Fig. 3). Both HBNs in active site of $\beta$-lactamase protein are represented with analogous circuit depicted on Fig. 6. This circuit could be considered as "integrated" circuit built of molecules.

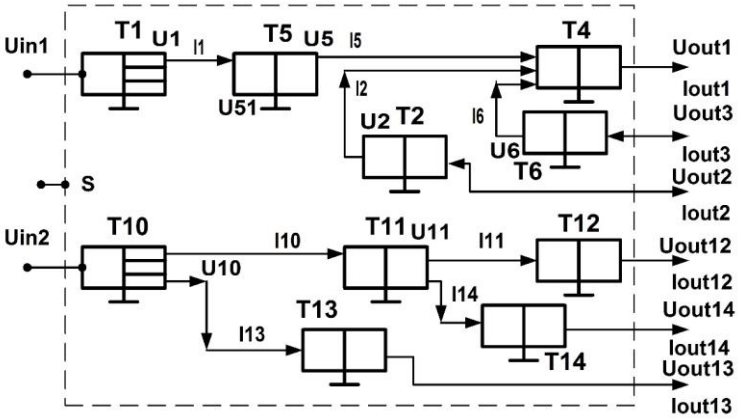


**Fig. 6** Correspondence between protein residues and water molecules in EY case and respective block–elements: in K73 and K234 correspond to T1 and T10 block-elements (i.e. they are circuit inputs), E166 → T4 ($U_{out1}$), N170 and W297 → T2, N132 → T5, N170 → T6, D214 → T12, S130OG → T13, S235OG → T14

Subject of the modeling effort is to describe the HBN in the active site of $\beta$-lactamase protein; the equivalent circuit of the hydrogen bonding network is given in Fig. 6 which is analogous to the circuit on Fig. 3 (EY). The equivalent circuit consists of two subcircuits corresponding to the respective nucleophilic and electrophilic HBN of the acyl enzyme (EY). Proton transfer depends on pH of the environment and the interaction of enzyme with ligand. Therefore, the two circuits are bound together in common circuit (which can be considered as **"integrated" circuit**) and cannot be separated. The ligand is represented in the equivalent circuit by the switch S – the switching of elements and the change of I/O currents depends on the position of S; by the position of the switch in fact we may select the intermediates of the acyl enzyme reaction. It should be noted that the ligand formation and its charge in active site, strongly affects proton transfer through the HBNs.

The output of the first electric circuit is denoted with Uin1; this circuit is analogous to the nucleophilic HBN. T1 block-element corresponds to K73NZ lysine which here behaves as proton donor and that is why it is interpreted as current source in the circuit; T1 has equal input and output voltages but different input and output currents. T2 substitutes the water molecule W297. Here we do not have a block-element designated by "T3" because we examine the last intermediate of the acylenzyme reaction where the S70OG residue has already completed the reaction and we reassign T2 to represent the water molecule; in the other intermediate of the reaction the water molecule is represented by T3 block-element but now there is no S70 residue we reassign the number for the water molecule block-element. T4 is juxtaposed to E166 which is proton acceptor and can form different hydrogen bonds; T4 sums three input currents. T5 and T6 block-elements are analogous

to N132 and N170 asparagines, respectively. Aspargines can be both donors and acceptors and thence they can alter the current direction; in the circuit, this is modeled by the S switch (S corresponds to the ligand).

The input of the second electric circuit is denoted by $U_{in2}$; this circuit is analogous to electrophilic HBN. T10 block-element corresponds to K234NZ proton donor. It is a current source (similarly to the current source T1 in the first electric circuit) and again it has equal input and output voltages but different input and output currents. T11 is analogous to the water molecule W309. T12 is juxtaposed to D214 residue which is in fact output of the circuit. T13 represents S130OG residue – it has equal input and output voltages but different input and output currents. T14 is the other output of the circuit; it is compared to S235OG residue and has the same properties as S130OG.

### 3.2. Equation formulation

The *I-V* characteristics of block-elements that correspond to proton transfer parameter and electrostatic potential of hydrogen bonds are coded in Matlab. Because the acyl reaction goes together with proton transfer, the proton transfer through each hydrogen bond in each reaction intermediate is simulated. This proton transfer is also compared to the current flow through known electronic elements.

The relations between currents and voltages of each block-element in the equivalent circuit are given by polynomials.

First, we list the equations for nucleophilic subcircuit. Equations (3) and (4) describe voltage and current of first output of T1 (the input voltage $U_{in}$ is between –2.3 ÷ +2.2 V):

$$U_{in} = U_1 \tag{3}$$

$$I_1 = 3*10^{-5}U_1^{\,2} + 0.0004U_1 + 0.0045 \tag{4}$$

The *I-V* equations for T5 are:

$$U_{51} = 0.0516U_1 - 0.2473 \tag{5}$$

$$U_5 = 1.0595U_{51} - 0.242 \tag{6}$$

$$I_5 = -3*10^{-6}U_5^{\,4} + 5.5*10^{-6}U_5^{\,3} + 2*10^{-5}U_5^{\,2} - 5*10^{-5}U_5 + 1.2*10^{-4} \tag{7}$$

T2 block-element is modeled by:

$$U_2 = 1.0211U_1 - 0.1005 \tag{8}$$

$$I_2 = = -1.0658U_2^{\,3} - 0.1179U_2^{\,2} + 10.912U_2 + 151.84 \tag{9}$$

Voltage and current of T6, which is output No. 3 of the circuit, are:

$$U_6 = 1.1204U_1 - 0.3978 \tag{10}$$

$$I_6 = 0.0045U_6^{\,2} + 0.0139U_6 + 0.0251 \tag{11}$$

T4 that is output No. 1 of the circuit is described by

$$U_4 = 1.0732U_2 - 0.1933 \tag{12}$$

The current of T4 is a sum of all input current:

$$I_4 = I_3 + I_5 + I_6 = I_{out1} \tag{13}$$

The equations for electrophilic subcircuit of HBNs are listed below. T10 block-element is modeled by:

$$U_{10} = 0.9658U_1 + 0.2266 \tag{14}$$

$$I_{10} = -0.0062U_{10}^3 - 0.002U_{10}^2 + 0.0751U_{10} + 0.5283 \tag{15}$$

The *I-V* characteristics of T11 are:

$$U_{11} = 1.002U_{10} + 0.1153 \tag{16}$$

$$I_{11} = -3*10^{-6}U_{11}^5 + 9*10^{-6}U_{11}^4 + 1.7*10^{-5}U_{11}^3 - 4*10^{-5}U_{11}^2 - 9.2*10^{-5}U_{11}^2 + 0.00025 \tag{17}$$

For T12, which is circuit output No. 12, we have:

$$U_{12} = 0.9904U_{11} + 0.4309 \tag{17}$$

$$I_{12} = I_{11} \tag{18}$$

Circuit output No. 13 is described by :

$$U_{13} = 1.0318U_{10} - 0.1714 \tag{19}$$

$$I_{13} = 0.0008U_{13}^3 - 0.0018U_{13}^2 - 0.0001U_{13} + 0.0042 \tag{20}$$

The last output, No. 14, is modeled by:

$$U_{14} = 1.01U_{11} - 0.1509 \tag{21}$$

$$I_{14} = -0.0431U_{14}^4 + 0.1242U_{14}^3 + 0.1987U_{14}^2 - 0.1987U_{14} + 12.893 \tag{22}$$

### 3.3. Matlab code

Below we list an excerpt of the Matlab code used to model the equivalent circuit behavior:

```
% block T14(s235) OUT14-> 1inp=1out Arguments
% function  -> 1inp-1out
% equation for U114 = F(U11)
U14 = 1.01*U11 -0.1509;

plot(U11,U14,'linewidth',2);
set(gca,'fontweight','b','fontsize',14)
grid on
title('T14 OUT14');
xlabel('U11 [V]');
ylabel('Uout14 [V]');
legend('simulation','data');
set(legend('simulation','data',1),'fontsize',12);
pause;

% Equation for I14=f(U14) inp1=out1
I14 = -0.0431*U14.^4 +0.1242*U14.^3 +0.1987*U14.^2 -0.1987*U14 +12.893;

plot(U14,I14,'linewidth',2);
set(gca,'fontweight','b','fontsize',14)
grid on
```

```
title('T14 OUT14');
xlabel('Uout14 [V]');
ylabel('Iout14 [pA]');
legend('simulation','data');
set(legend('simulation','data',1),'fontsize',12);
pause;

% % % ++++++++++++++++++++++++++
plot(U7,I51,'-r',U7,I7,'--b','linewidth',2);
set(gca,'fontweight','b','fontsize',14)
grid on
title('I51, I7 vs U7');
xlabel('U7 [V]');
ylabel('I51, I7 [pA]');
set(legend('I51','I7',12),'fontsize',12);
h = legend('cos','sin',2);
pause;
```

## 4. Simulation Results and Discussion

We perform DC and transient analyses to study circuit behavior in different modes of operation in Matlab.

### 4.1. DC analysis

The DC analysis is carried out by sweeping input voltage between –2.3 and +2.2 V. The simulated results with the above polynomial equations are compared to the results of [24] (cf. Fig. 7). It is observed that the polynomials well describe the behavior of the modeled block-elements. We observed similar results for the rest of the block-elements (we do not show them here). The maximal error is 5.66 %.

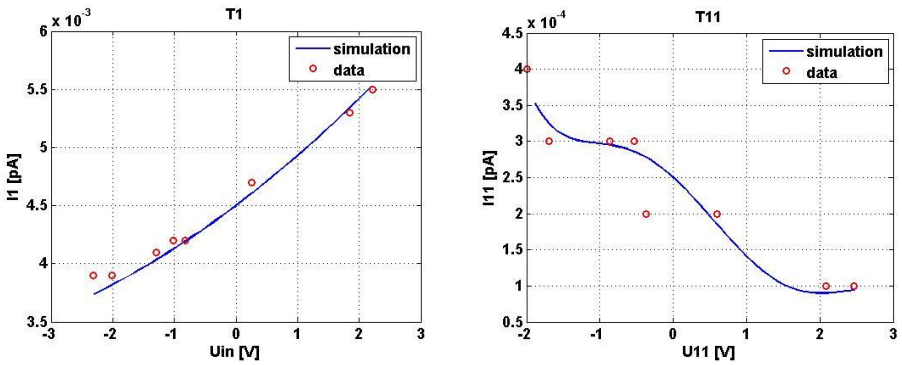


**Fig. 7** *I-V* characteristics of block-elements T1 and T11 (representing K73 and w309) for (EY) intermediate of the acylenzyme reaction

Next, we perform static analysis of the equivalent circuit (Fig. 6). The simulated *I-V* characteristics are illustrated in Figures 8, 9, 10, 11, 12, and 13.

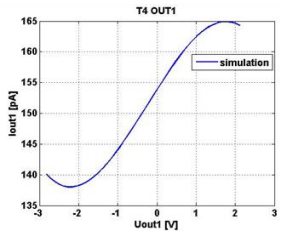


**Fig. 8** $I_{out1}$ vs. $U_{out1}$

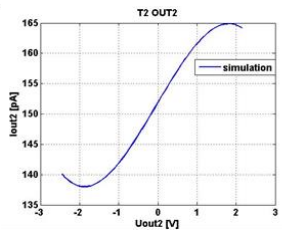


**Fig. 9** $I_{out2}$ vs. $U_{out2}$

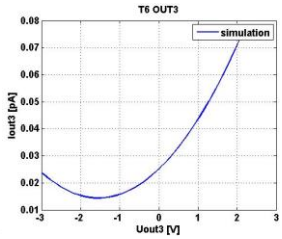


**Fig. 10** $I_{out3}$ vs. $U_{out3}$

Simulation results show S-type form of the outputs characteristics (in Fig. 10 the form is similar to an exponent) which implies that the circuit can operate as an **amplifier**.

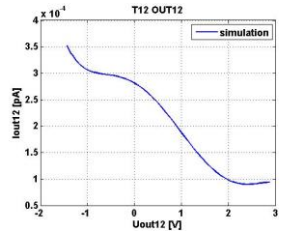


**Fig. 11** $I_{out12}$ vs. $U_{out12}$

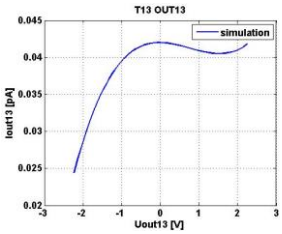


**Fig. 12** $I_{out13}$ vs. $U_{out13}$

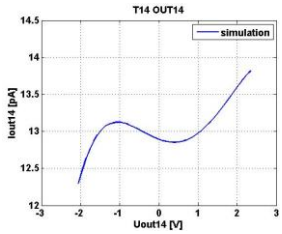


**Fig. 13** $I_{out14}$ vs. $U_{out14}$

The *I-V* characteristic in Fig. 11 cannot be directly compared to a common microelectronic device. Conversely, in Fig. 12 the current exhibits two regions: 1) $I_{out13}$ increases almost linearly and then 2) $I_{out13}$ saturates, hence the characteristic is analogous to the *I-V* characteristics of a **transistor**. In Fig. 13 we observe a characteristic that is typical for a **tunnel diode**.

We also simulated the dependence of output voltages versus input voltage. The results showed that all output voltages are *linearly* increasing with the input voltage.

### 4.2. Dynamic analysis

Taking into account the specifics of the hydrogen bonding networks and the proton transfer, which takes place for a period of approximately $10^{-11}$ s, the analogous electronic circuit should transfer signals in the GHz-range. That is why, we begin with input voltage with amplitude between –2.2 and +2.2 V at frequency of 10 GHz and a time sweep between 0 and 0.1 ns. Afterwards, we feed input voltages with positive amplitude only and then with negative amplitude only (Fig. 14).

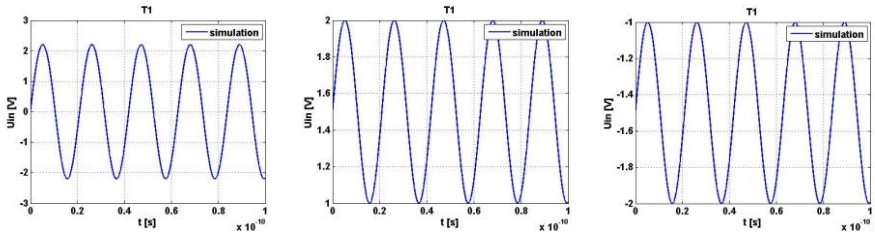


a) $U_{in}$ = 2.2×sin(5×10$^{11}$×t) b) $U_{in}$ = 1 +sin(5×10$^{11}$×t) c) $U_{in}$ = –1 +sin(5×10$^{11}$×t)

**Fig. 14** $U_{in}$ vs. time

In Fig. 15 we show the characteristics of T4 block-element which is output No. 1 of the nucleophilic circuit.

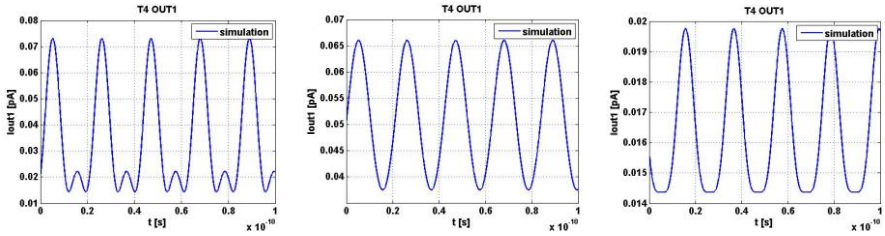


a) $U_{in}$ = 2.2×sin(5×10$^{11}$×t) b) $U_{in}$ = 1 +sin(5×10$^{11}$×t) c) $U_{in}$ = –1 +sin(5×10$^{11}$×t)

**Fig. 15** $I_{out1}$ vs. time at different input voltages

The results show that $I_{out1}$ is always positive regardless of whether the input voltage is positive and negative, positive only, or negative only. In the case of Fig. 15a) we observe that the signal $I_{out1}$ at is cut from the bottom. Therefore, we can compare the results to the characteristics of a **signal limiter**.

In Fig. 16 we show the characteristics of T2 block-element which is output No. 2 of the nucleophilic circuit.

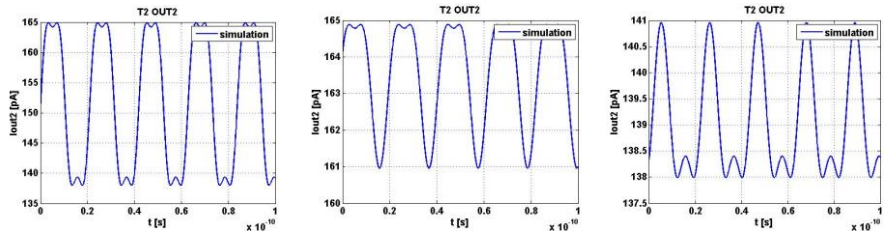


a) $U_{in}$ = 2.2×sin(5×10$^{11}$×t) b) $U_{in}$ = 1 +sin(5×10$^{11}$×t) c) $U_{in}$ = –1 +sin(5×10$^{11}$×t)

**Fig. 16** $I_{out2}$ vs. time at different input voltages

We observe that the sine output characteristic in Fig. 16a) is cut from the top and bottom, in Fig. 16b) – from the top, and in Fig. 16c) – from the bottom.

In Fig. 17 we show the characteristics of T6 block-element which is output No. 3 of the nucleophilic circuit.

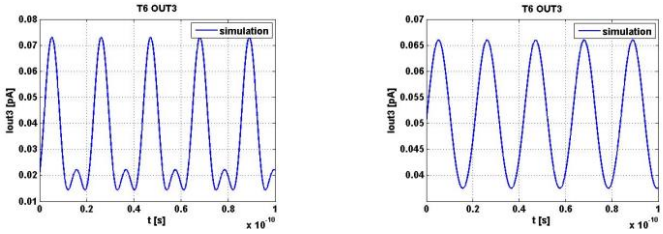


a) $U_{in} = 2.2 \times \sin(5 \times 10^{11} \times t)$ b) $U_{in} = 1 + \sin(5 \times 10^{11} \times t)$

**Fig. 17** $I_{out3}$ vs. time at different input voltages

Fig. 18 gives the characteristics of T12 block-element which is output No. 12 of the electrophilic circuit.

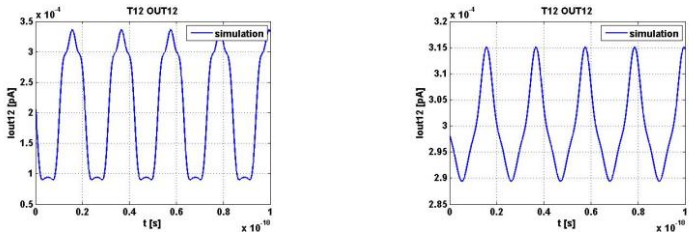


a) $U_{in} = 2.2 \times \sin(5 \times 10^{11} \times t)$ b) $U_{in} = 1 + \sin(5 \times 10^{11} \times t)$

**Fig. 18** $I_{out12}$ vs. time at different input voltages

In Fig. 19 we present the characteristics of T13 block-element that is output No. 13 of the electrophilic circuit.

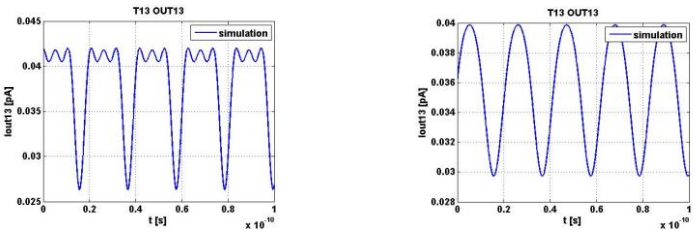


a) $U_{in} = 2.2 \times \sin(5 \times 10^{11} \times t)$ c) $U_{in} = -1 + \sin(5 \times 10^{11} \times t)$

**Fig. 19** $I_{out13}$ vs. time at different input voltages

Fig. 20 shows the characteristics of T14 block-element which is output No. 14 of the electrophilic circuit.

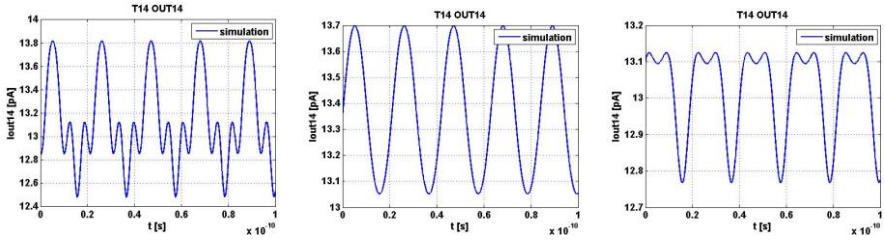


a) $U_{in} = 2.2 \times \sin(5 \times 10^{11} \times t)$ b) $U_{in} = 1 + \sin(5 \times 10^{11} \times t)$ c) $U_{in} = -1 + \sin(5 \times 10^{11} \times t)$

**Fig. 20** $I_{out14}$ vs. time at different input voltages

The signal in Fig. 21a) indicates **modulator**'s nature – the output signal is modulated.

From transient analyses, we obtain characteristics that can be compared to amplitude limiter, modulator and triangular pulse source.

## 5. CONCLUSION

The presented circuit model of hydrogen bonding networks in the active site of $\beta$-lactamase protein proved that such biofunctional system exhibits properties that are akin to common microelectronic devices. The analogous microelectronic circuit may operate in static mode as a signal amplifier, transistor or tunnel diode. In dynamic mode, the microelectronic circuit may operate as signal limiter or signal modulator in the GHz-range. Furthermore, signals with different frequency, amplitude, and width might be generated at each circuit output.

Thus, it can be concluded that the electrophilic and nucleophilic networks of hydrogen bonds in the active site can operate like an integrated circuit consisting of individual devices in the form of hydrogen bonds. The biocircuit is extremely flexible and it is applicable to multiple circuit purposes.

The results are expected to have important applications for finding novel solutions in bioelectronics research.

**Acknowledgement**: *The present paper is a part of the research carried out in the framework of project ДУНК 01/03 of 29.12.2009.*

## REFERENCES

[1] K. Habermüller, M. Mosbach, and W. Schuhmann, "Electron-Transfer Mechanisms in Amperometric Biosensors," *Fresenius' Journal of Analytical Chemistry*, Vol. 366, No. 6-7, 2000, pp. 560-568.

[2] A. Heller, "Electrical connection of enzyme redox centers to electrodes", *Acc. Chem. Res.*, 23, pp. 128–134, 1990.

[3] F.A. Armstrong and G.S. Wilson, "Recent developments in faradaic bioelectrochemistry", *Electrochim. Acta* 45 (15-16), pp. 2623-2645, 2000.

[4] C. Dekker and M.A. Ratner, "Electronic properties of DNA", *Physics World*, 14 (8), pp. 29-33 August 2001.
[5] A. Heller, "Miniature biofuel cells", *Phys. Chem. Chem. Phys.*, 6, pp. 209–216, 2004.
[6] E. Katz, A.N. Shipway, I. Willner, in *Handbook of Fuel Cells – Fundamentals, Technology, Applications* (Eds.: W. Vielstich, H. Gasteiger, A. Lamm), vol. 1, part 4, Wiley, Chichester, Chapter 21, pp. 355–381, 2003.
[7] P. Fromherz, "Electrical Interfacing of Nerve Cells and Semiconductor Chips", *Chem. Phys. Chem.*, 3, pp. 276-284, 2002.
[8] M. Baca, G, Borgstahl, M. Boissinot, P. Burke, D. Williams, K. Slater, E. Getzoff, "Complete chemical structure of photoactive yellow protein: novel thioester-linked 4-hydroxyxinnamyl chromophore and photocycle chemistry", *Biochemistry*, 33, pp. 14369–14377, 1994.
[9] H. Zhang, Q. Sun, Z. Li, S. Nanbu, S.S. Smith, "First principle study of proton transfer in the green fluorescent protein (GFP): Ab initio PES in a cluster model", *Computational and Theoretical Chemistry*, 990, pp. 185–193, 2012.
[10] K. J. Wise, N. B. Gillespie, J. Stuart, M. P. Krebs, and R. R. Birge, "Optimization of bacteriorhodopsin for bioelectronic devices", *Trends in Biotechnology*, vol. 20, no. 9, pp. 387–94, September 2002.
[11] R.A. Marcus, N. Sutin, "Electron transfers in chemistry and biology", *Biochim. Biophys. Acta*, 811, pp. 265–322, 1985.
[12] M. Bixon, J. Jortner, "Electron transfer. From isolated molecules to biomolecules", *Adv. Chem. Phys.*, 106, pp. 35–202, 1999.
[13] H.B. Gray, J.R.Winkler, "Electron tunneling through proteins", *Q. Rev. Biophys.*, 36, pp. 341–372, 2003.
[14] F.K. Majiduddin, I.C. Materon, T.G. Palzkill, "Molecular analysis of beta-lactamase structure and function", *International Journal of Medical Microbiology*, vol. 292, iss. 2, pp. 127-137, 2002.
[15] M.A. Lill and V. Helms, "Compact parameter set for fast estimation of proton transfer rates", *J. Chem. Phys.*, vol. 114 (3), p.1125-1132, 2001.
[16] R. Rusev, G. Angelov, T. Takov, M. Hristov, "Biocircuit for Signal Modulation Based on Hydrogen Bonding Network", *Annual J. of Electronics*, vol. 3, no. 2, pp. 155-158, 2009.
[17] R. Rusev, G. Angelov, B. Atanassov, T. Takov, M. Hristov, "Development and Analysis of a Signal Transfer Circuit with Hydrogen Bonding", *In Proc. of the 17th Intl. Scientific and Appl. Science Conf. (ELECTRONICS ET'2008)*, Sozopol, Bulgaria, Book 4, September 2008, pp. 37-42.
[18] R. Rusev, G. Angelov, T. Takov, B. Atanasov, M. Hristov, "Comparison of Branching Hydrogen Bonding Networks with Microelectronic Devices", *Annual J. of Electronics*, vol.3, no. 2, pp. 152-154, 2009.
[19] R. Rusev, G. Angelov, E. Gieva, T. Takov, M. Hristov, "Hydrogen Bonding network as a DC Level Shifter and a Power Amplifier", *In Proc. of 17th Intl. Conf. Mixed Design of Integrated Circuits and Systems (MIXDES 2010)*, Wroclaw, Poland, June 24-26, 2010, pp. 408-411.
[20] R. Rusev, G. Angelov, E. Gieva, M. Hristov, T. Takov, "Hydrogen bonding network emulating frequency driven source of triangular pulses", International Journal of Microelectronics and Computer Science, vol. 1, no. 3, pp. 293-298, 2010.
[21] E. Gieva, L. Penov, R. Rusev, G. Angelov, M. Hristov, "Protein Hydrogen Bonding Network Electrical Model and Simulation in Verilog-A", Annual J. of Electronics, vol.5, no. 2, pp. 132-134, 2011.
[22] B. Atanasov, D. Mustafi, M. Makinen, "Protonation of the $\beta$-lactam nitrogen is the trigger event in the catalytic action of class A $\beta$-lactamases", *Proc. Natl. Acad. Sci*., USA, 97 (7), p. 3160-3165, 2000.
[23] Matlab website http://www.mathworks.com/
[24] R. Rusev, G. Angelov, E. Gieva, B. Atanasov, M. Hristov, "Microelectronic Aspects of Hydrogen Bond Characteristics in Active Site of $\beta$-lactamase during the Acylenzyme Reaction", *Annual J. of Electronics*, Vol. 6, No. 2, pp. 35-38, 2012.